Deeply Virtual Compton Scattering at HERA

Rainer Stamen*
on behalf of the H1 and ZEUS Collaborations

*Universität Dortmund[1]
Germany
IIHE–Université Libre de Bruxelles
Belgium

Abstract. Measurements of Deeply Virtual Compton Scattering at the ep collider HERA by the H1 and ZEUS Collaborations are presented and the cross section is shown as a function of Q^2 and W. The results are compared to LO QCD calculations based on the two gluon exchange model.

INTRODUCTION

Deeply Virtual Compton Scattering (DVCS) [1,2] is the hard diffractive scattering of a virtual photon off a proton. The QCD interpretation of this process, based on the two gluon exchange model, is shown in figure 1. The virtual photon emitted by the incoming electron interacts via a quark loop with two gluons from the proton resulting in a proton, a photon and an electron in the final state.

DVCS offers a new and comparatively clean way to study diffraction at HERA. In comparison to vector-meson production it is free from the large uncertainties on the vector-meson wave-function. The largest interest arises from the access it may provide experimentally to the skewed parton distributions of the proton [3].

DVCS contributes to the reaction $e^+p \longrightarrow e^+\gamma p$, whose total cross section is dominated by the purely electromagnetic Bethe–Heitler process[2] where the final state photon originates from initial or final state radiation off the in– or outgoing electron. The diagrams of this process are shown in figure 2.

In the presence of a large scale the DVCS process can be calculated in perturbative QCD. In the present case the scale is given by the photon virtuality Q^2 which is above a few GeV^2. It has been shown that for the DVCS process factorisation

---

1) This work was supported by the Graduiertenkolleg Elementarteilchenphysik of the Deutsche Forschungsgemeinschaft at the Universität Dortmund, the Deutscher Akademischer Austauschdienst, Bonn and the Martin Schmeißer Stiftung at the Universität Dortmund

2) also called QED Compton process

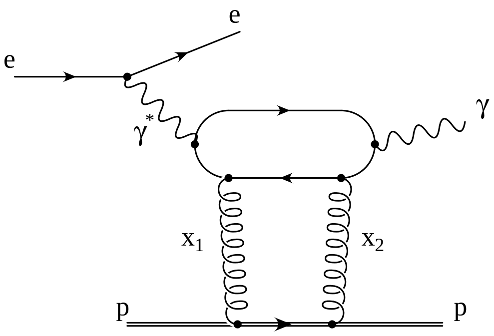

FIGURE 1. DVCS diagram in the QCD picture.

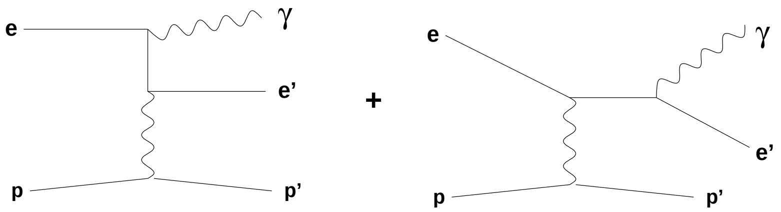

FIGURE 2. LO Diagrams contributing to the Bethe–Heitler process.

holds which means that the scattering amplitude factorises in a hard scattering part which can be calculated in perturbative QCD and a parton density which absorbs non–perturbative effects [4]. In a naive model the gluon content of the proton can be modeled by using the square of the ordinary gluon distribution $|xg(x, Q^2)|^2$ in the calculations. Since for the DVCS process the virtual photon is scattered onto mass shell in the final state, it is necessary to transfer longitudinal momentum from the photon to the proton, i.e. forcing a non–forward kinematic situation. In the picture of the two gluon exchange the fractional momenta of the gluons x_1 and x_2 are therefore not equal which leads to the concept of skewed parton distributions [3].

LO QCD calculations, based on the two gluon exchange model exist [2]. These calculations, including the interference between the DVCS and the Bethe–Heitler process, are embedded in two independent MC generators used by the two experiments at the HERA *ep* collider. The DVCS process provides in principle the possibility to extract these distributions from experimental data [5].

ANALYSIS STRATEGY

Around the interaction region both experiments, H1 [6] and ZEUS [7], are equipped with tracking devices which are surrounded by calorimeters. Since the proton escapes the main detector through the beam pipe only the scattered electron and the photon are detected. Therefore the event selection is based on the requirement of two electromagnetic clusters, one in the backward and one in the central or forward part of the detector where the backward direction is defined as the direction of the incoming electron. No other cluster above a certain noise threshold must be found in the calorimeter.

If a track can be reconstructed in the event it has to be associated to one of the clusters and determines the electron candidate. To enhance the DVCS contribution w.r.t. the Bethe–Heitler process the phase space is restricted by requiring the photon candidate in the forward or central part of the detector. In case of the H1 analysis the elastic component is specifically selected by additional use of the forward detectors placed close to the beam pipe in order to identify particles originating from proton dissociation processes.

ZEUS RESULTS

The ZEUS analysis [8] is based on a luminosity of $37.5\,\mathrm{pb}^{-1}$ taken in the 1996/97 data taking period. A photon virtuality $Q^2 > 6\,\mathrm{GeV}^2$ is demanded. In figure 3a the polar angular distribution of the electron and photon candidates measured in the central part of the calorimeter is shown. A clear signal above the expectations for the Bethe–Heitler process is observed. If one takes the full calculations including the DVCS process a good description of the experimental data is achieved. Figure 3b shows the polar angular distribution for the photon candidates only. Here the difference between the data and the expectation for the Bethe–Heitler process is larger since the photon is more likely to be found in the central part for the DVCS process than for the Bethe-Heitler process. This can also be seen in figure 3c which shows the angular distribution of the ratio of the number of photon candidates over the sum of photon and electron candidates. If the photon energy cut is increased from 2 to 5 GeV, the clear signal persists (not shown). In all cases the data are quite well described by the Monte Carlo model.

As a cross check a shower shape analysis has been performed showing that the signal originates from single photons and not from π^0 background which could arise from low multiplicity hadron production. Such processes are included in commonly used DIS MC generators. Since these processes have, however, never been explicitly measured at HERA energies the predictions of the available MC programs, tuned for high multiplicity events, are unreliable. Hence π^0 background has been studied using real data.

A cluster shape analysis is performed using the variables $\mathrm{Z_{width}}$ and $\mathrm{f_{MAX}}$, where $\mathrm{Z_{width}}$ is the energy weighted sum over all distances z between each cluster cell and the reconstructed center of the electromagnetic cluster; $\mathrm{f_{MAX}}$ represents the fraction of energy in the most energetic cell w.r.t. the total energy of the cluster. Since the π^0 decays into two photons with a finite opening angle, a broader distribution of the variable $\mathrm{Z_{width}}$ is expected compared to single photons. For the same reason the variable $\mathrm{f_{MAX}}$ should be well below one for π^0 induced clusters whereas for single

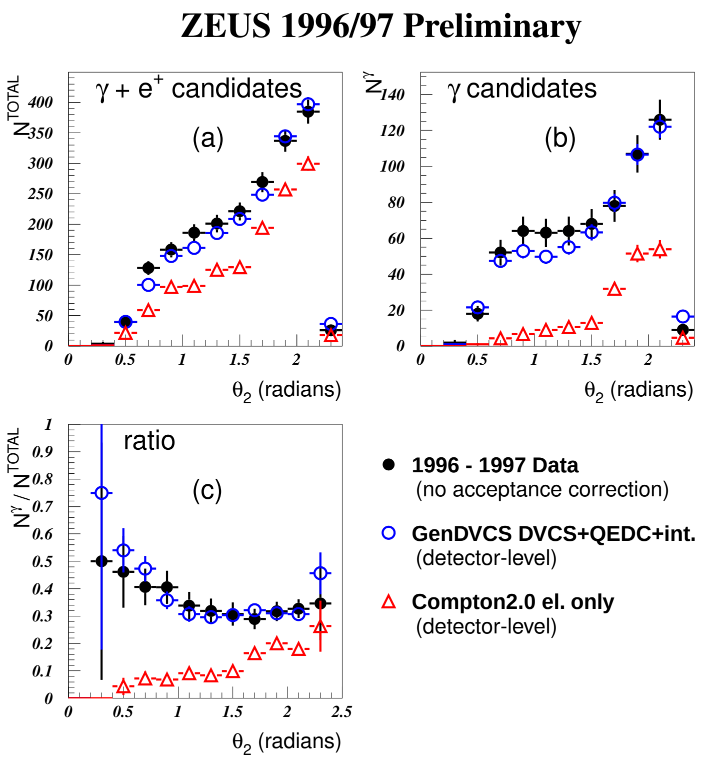

FIGURE 3. (a) Distribution of the polar angle of the photon and electron candidates in the central part of the calorimeter with an energy $E > 2\,\mathrm{GeV}$; (b) the polar angle of the photon candidates with no track associated with the electromagnetic cluster; (c) the ratio of the distributions in (b) and (a). The data are shown as solid points; the (DVCS + QEDC + Int.) MC prediction is shown as open circles and the one from the QED Compton MC as open triangles.

photons a value close to one is expected.

The results of these studies are summarised in figure 4. The data are compared to the MC prediction of the full QCD calculation and to the predictions from the RAPGAP [10] and the DJANGOH [11] programs. In figure 4 a) and b) the angular distributions for the photon candidates are shown. For the shower shape analysis only candidates with $\theta_2 < 1.5$ are used where the DVCS contribution to the cross section is expected to dominate. The resulting distributions for the shower shape variables are shown in figures 4 c)–f) and compared to the different MC predictions. A good description of the distributions by the DVCS MC is achieved while the π^0 prediction differs significantly from the data indicating that the data cannot be explained as hadronic background from low–multiplicity DIS events.

H1 RESULTS

The H1 analysis [9] is based on a luminosity of $8\,\mathrm{pb}^{-1}$ taken in the 1997 data taking period. The event sample was divided into two parts:

- A **control sample** where the electron is required to be in the central part of the detector. The electron is identified by a track measured with the central tracking system associated to an electromagnetic cluster in the fine grained calorimeter.

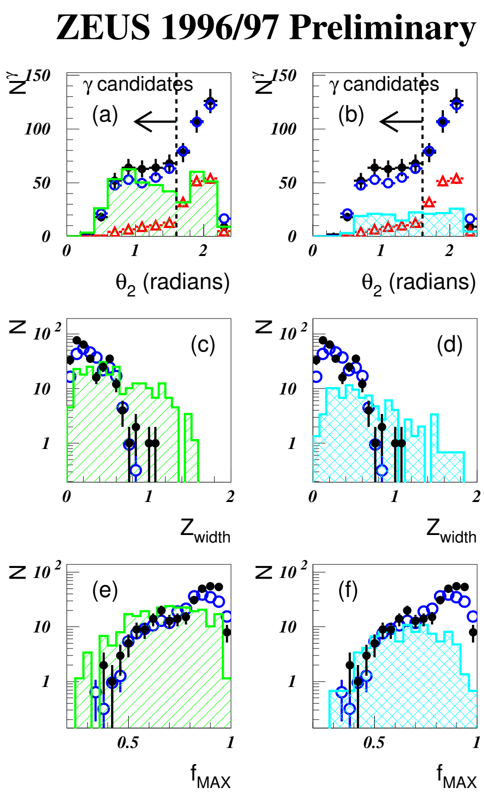

FIGURE 4. (a,b) Distribution of the polar angle of the photon candidates with an energy $E > 2\,\mathrm{GeV}$; (c,d) distribution of the variable $\mathrm{Z_{width}}$, expressed in units of the BCAL EMC cell width and (e,f) distribution of variable $\mathrm{f_{MAX}}$. The ZEUS data are shown as solid points; the (DVCS + QEDC + INT) MC simulated events are shown as open circles; the QEDC Monte Carlo simulated events are shown as open triangles. In (a,c,e) the data are compared to a low-multiplicity Monte Carlo simulated sample from DJANGOH, while (b,d,f) show the comparison with RAPGAP-generated events. The MC predictions are normalised to the same luminosity as the data.

- A **signal sample** where the photon is required to be in the central part of the detector. Here the photon is identified by the absence of a track in front of the electromagnetic cluster measured in the calorimeter.

The control sample is dominated by the Bethe–Heitler process, while the DVCS contribution is negligible. In addition two further processes were found to contribute to this event signature: the diffractive production of ρ-mesons and the elastic dilepton production. Both processes contribute if one of the outgoing particles leaves the main detector through the beam pipe. The processes have been studied using the DIFFVM [13] and GRAPE [14] MC programs respictively. In figure 5, the uncorrected event distributions are seen to be well described by the sum of the three MC predictions, assuring that the detector response is well understood.

The acceptance, initial state radiation of real photons and detector effects have been estimated by MC to extract the elastic $e^+p \longrightarrow e^+\gamma p$ cross section which has been measured in the kinematic region $2 < Q^2 < 20\,\mathrm{GeV}^2$, $|t| < 1\,\mathrm{GeV}^2$ and $30 < W < 120\,\mathrm{GeV}$ using the signal sample. The event kinematics is calculated using the measured angles of the final state electron and photon. The proton dissociation background is estimated to 10% and has been subtracted. The main systematic error arises from the measurement of the polar angles of the electron and photon used to determine the kinematics. The full error is however dominated by the limited statistics.

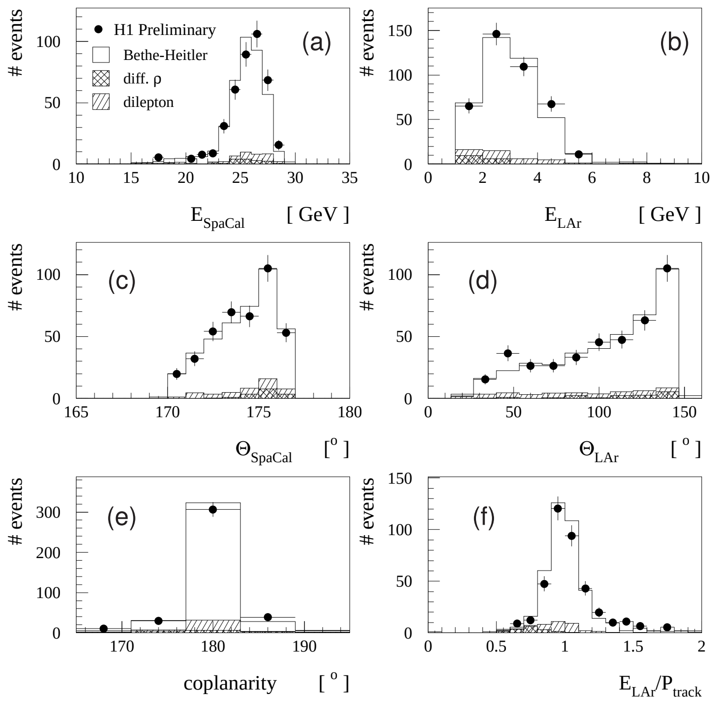

FIGURE 5. Event distributions (uncorrected) of the control sample (see text). The data are compared to the sum of the prediction for the Bethe–Heitler process, elastic dilepton production and diffractive ρ–production. (a) energy of the cluster in the backward calorimeter (SpaCal), (b) energy of the cluster in the central calorimeter (LAr), (c) polar angle of the cluster in the SpaCAL, (d) polar angle of the cluster in the LAr calorimeter, (e) coplanarity, i.e. the difference in the azimuthal angle of the two clusters, (f) ratio of the energy of the cluster and the momentum measured by the tracking detector for the electron candidate.

Figures 6 and 7 show the $e^+p \longrightarrow e^+\gamma p$ differential cross section as a function of Q^2 and of W. The data are compared with the Bethe–Heitler prediction alone and with the full calculation including Bethe–Heitler and DVCS. One finds a good description of the data by the full calculations.

Finally it must be noted that the t-slope cannot be calculated at low t leading to a free parameter in the theory which can only be extracted from experimental data. This has not yet been done. In the QCD comparisons the t dependence is assumed to be $e^{-b|t|}$. The free parameter b leads mainly to a normalisation uncertainty of the prediction. In the figures the t-slope b is assumed to be between 7 and 10 GeV^{-2}. Hence the data should be compared to the prediction only w.r.t. the shape and the absolute normalisation should be taken with care.

CONCLUSION

The DVCS process has been observed by the H1 and ZEUS Collaborations and the first $e^+p \longrightarrow e^+\gamma p$ cross section measurement has been presented. The experimental results are well described by the LO QCD calculations of Frankfurt et al. [2] although a dedicated t-slope measurement is needed to determine the normalisation for the calculations.

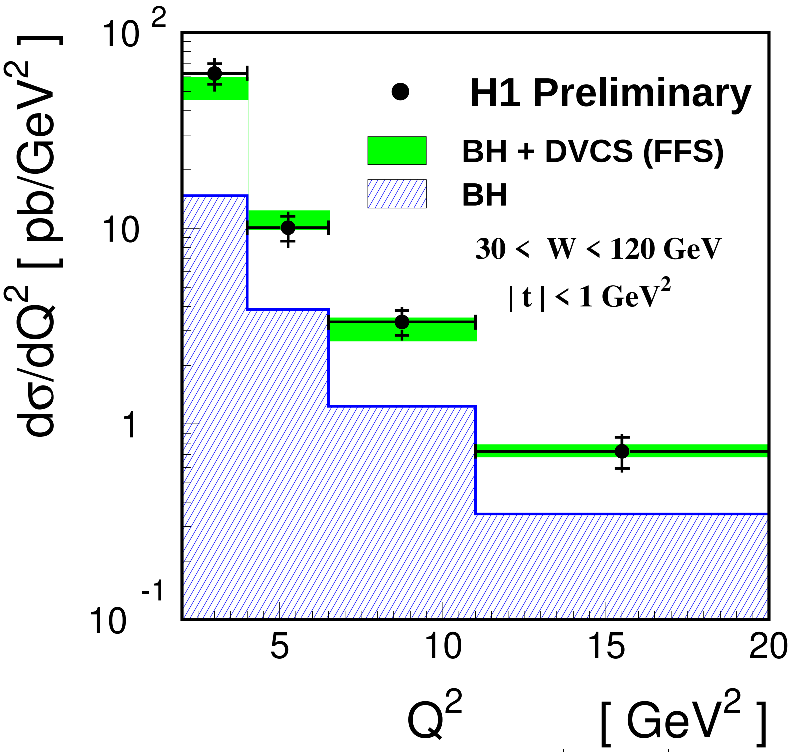

FIGURE 6. The measured cross sections of the reaction $e^+p \longrightarrow e^+\gamma p$ as a function of Q^2 is shown and compared to theoretical prediction (FFS)[2] (shown as band). The cross section is measured in the kinematic range $30 < W < 120\,\mathrm{GeV}$, $|t| < 1\,\mathrm{GeV}^2$. The uncertainty in the theoretical prediction for the DVCS process is dominated by the unknown slope of the t-dependence of the DVCS part of the cross section, assuming $7 < b < 10\,\mathrm{GeV}^{-2}$. In addition the prediction for the Bethe–Heitler process is shown separately (hatched).

REFERENCES

1. X. Ji, Phys. Rev. **D55**(1997) 7114.
2. L. L. Frankfurt, A. Freund, M. Strikman, Phys. Rev. **D58** (1998) 114001 and erratum Phys. Rev. **D59** (1999) 119901E.
3. A. V. Radyushkin Phys. Rev. **D56** (1997) 5524.
4. J. C. Collins, A. Freund, Phys. Rev. **D59**(1999) 074009.
5. A. Freund, Phys. Lett. **B 472** (2000) 412.
6. H1 Collaboration, I. Abt et al., *Nucl. Instrum. Methods* A **386** (1997) 310 and 348.
7. ZEUS Collab., M. Derrick *et al.* Status Report 1993, DESY (1993).
8. P. R. B. Saull, hep-ex/0003030 and ZEUS Collab., paper cont. EPS 99 `http://www-zeus.desy.de/~schlenst/eps99_paper.html`.
9. H1 Collab.,paper cont. ICHEP 2000, 966.
10. RAPGAP 2.08/00: H. Jung, Comp. Phys. Commun. **86** (1995) 147.
11. A. Kwiatkowski, H. Spiesberger and H. J. Möhring,

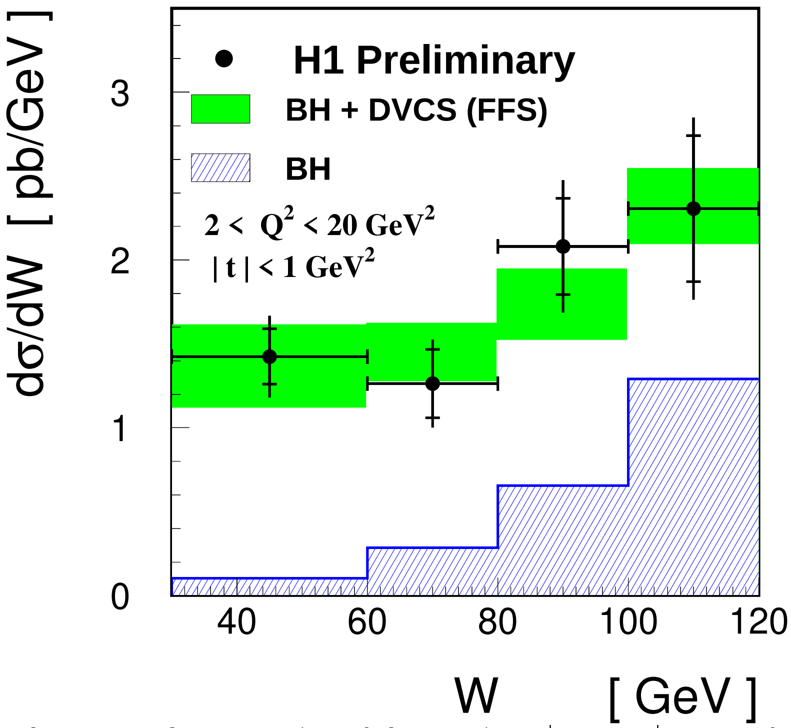

FIGURE 7. The measured cross section of the reaction $e^+p \longrightarrow e^+\gamma p$ as a function of W is shown and compared to the theoretical prediction (FFS)[2] (shown as band). The cross section is measured in the kinematic range $2 < Q^2 < 20\,\mathrm{GeV}^2, |t| < 1\,\mathrm{GeV}^2$. The uncertainty in the theoretical prediction for the DVCS process is dominated by the unknown slope of the t-dependence of the DVCS part of the cross section, assuming $7 < b < 10\,\mathrm{GeV}^{-2}$. In addition the prediction for the Bethe–Heitler process (BH) is shown separately (hatched).

Comp. Phys. Commun. **69** (1992) 155
K. Charchula,G. A. Schuler and H. Spiesberger,
Comp. Phys. Commun. **81** (1994) 381
DJANGOH version 1.1: H. Spiesberger, available from
`http://www.desy.de/~hspiesb/djangoh.html`.
12. A. Courau and P. Kessler, Phys. Rev. **D46** (1992) 117.
13. B. List, Diploma Thesis, Techn. Univ. Berlin, (1993).
14. T. Abe et al., in Proc. *Monte Carlo Generators for HERA physics*, Eds. A. T. Doyle, G. Grindhammer, G. Ingelman, H. Jung, DESY-PROC-1999-02, p. 566.